The Cryosphere Discuss., 4, 1741–1779, 2010
www.the-cryosphere-discuss.net/4/1741/2010/
doi:10.5194/tcd-4-1741-2010

The Cryosphere Discussions

The mass and energy balance of ice within the Eisriesenwelt cave, Austria

F. Obleitner[1] **and Ch. Spötl**[2]

[1]Institute of Meteorology and Geophysics, Innsbruck University, Austria
[2]Institute of Geology and Paleontology, Innsbruck University, Austria

Received: 14 September 2010 – Accepted: 15 September 2010
– Published: 23 September 2010

Correspondence to: F. Obleitner (friedrich.obleitner@uibk.ac.at)

Published by Copernicus Publications on behalf of the European Geosciences Union.

Abstract

Meteorological and glaciological measurements were performed in a prominent ice cave (Eisriesenwelt, Austria) during a full annual cycle. The observed meteorological conditions feature the basic characteristics of a dynamically ventilated cave system with a well distinguished winter and summer regime.

The calculated energy balance of the ice is largely predetermined by the input of long-wave radiation originating at the host rock surface. On average the turbulent fluxes withdraw energy from the surface. This is more pronounced during winter due to enhanced circulation and lower humidity. During summer the driving gradients reverse sign and the associated fluxes provide some energy for melt. About 4 cm of ice were lost at the measurements site during a reference year. This was due to some sublimation during winter, while the major loss resulted from melt during summer. Small amounts of accumulation occurred during spring due to refreezing of seepage water.

These results are largely based on employing a numerical mass and energy balance model. Sensitivity studies prove their reliability regarding diverse measurement uncertainties and indicate that the annual mass balance essentially depends on summer temperature and the availability of seepage water in spring. The latter induces a considerable interannual and spatial variability of the mass budget.

1 Introduction

The IPCC assessments highlighted the potential of terrestrial ice as a climate indicator. This is essentially true with respect to ice caps, glaciers and permafrost (Lemke et al., 2007). In contrast, the existence of ice within caves hardly gained scientific interest yet.

Ice caves are known from various climate regions and can be classified according to their thermal regime and the type of ice (Balch, 1900; Wigley et al., 1976; Silvestru, 1999; Luetscher and Jeannin, 2004). Some of them host substantial ice masses, served as natural storage rooms in the past (Canaval, 1893; Morton, 1962) or are major tourist attractions (e.g. Dachstein Rieseneishöhle, Eisriesenwelt).

Seven basic categories of cave ice can be distinguished depending on its appearance and the associated formation processes (Luetscher and Jeannine, 2004). The unique environmental conditions (no solar radiation, damped atmospheric signals, seepage water instead of atmospheric precipitation, no major mechanical stresses due to differential movements) result in specific physical and chemical ice properties (Citterio et al., 2004; Hausmann and Behm, 2010). Cave ice also bears a principal potential as a paleoclimate archive, which so far has been rarely touched upon due to dating problems (Silvestru, 1992; Holmlund et al., 2005; Luetscher et al., 2007; Kern et al., 2009; Stoffel et al., 2009; May et al., 2010). As far as can be judged from the sparse data available from alpine countries, the volume of cave ice has decreased in most caves during the past several decades (Luetscher et al., 2005; Erhard and Spötl, 2010). However, this trend cannot easily be related to climate change because of the complex processes within the soil-karst-cave system. Due to the lack of corresponding observations and models also the fate of cave ice in a global warming perspective remains largely unexplored. On the other hand there is some basic knowledge available on the meteorological and glaciological conditions in several alpine ice caves (e.g. Saar, 1956; Pavuza and Mais, 1999; Mais, 1999; Hausmann et al., 2010), while there are still only few studies on their energy and mass balance (Ohata et al., 1994a, b; Luetscher et al., 2008; Obleitner et al., 2009).

Eisriesenwelt (hereafter abbreviated as ERW) is a prominent cave located inside the Hochkogel Mountain at the western edge of Tennengebirge, Austria (47°30′ N; 13°11′ E). The cave has a total length of ca. 40 km with a lower entrance at 1641 m and probably several as yet unexplored upper entrances emerging at a karst plateau (ca. 2200 m). As a consequence of these multiple entrances ERW is a dynamically ventilated cave. Perennial ice only occurs within ca. 700 m behind the (lower) entrance; its total volume was estimated to ca. 30 000 m^3 distributed across an area of ca. 10 000 m^2. Historically, the meteorological and glaciological conditions in the cave were most intensively investigated in the 1920s (e.g. Hauser and Oedl, 1923) and in the 1950s (Gressel, 1955; Saar 1957) as reviewed by May et al. (2010). Notably, the show cave operators contributed a wealth of undocumented knowledge about ERW (A. Rettenbacher, F. Oedl; personal communications, 2010) and long-term temperature records at several sites along the ice-covered section. Unfortunately, these measurements were not carried out in a homogenous manner. Therefore, they are not suitable to evaluate eventual long-term trends, while Thaler (2008) revealed some basic features of the thermal regime inside the cave and its relationship to the outside environment. This paper focuses on the meteorological and glaciological conditions in the rear part of the ice covered section of ERW. Other aspects of this multidisciplinary research initiative are treated by Hausmann and Behm (2010), May et al. (2010) and Schöner et al. (2010). The data cover a full annual cycle and are used to drive a mass and energy balance model allowing enhanced evaluation of the inherent processes. Section 2 gives a detailed description of the environment at the measurement site, which is followed by a description of instrumentation (Sect. 3) and the model (Sect. 4). The results are discussed in Sect. 5 treating the meteorological and glaciological conditions, the calculated mass and energy balance and their sensitivity to diverse uncertainties and changes in atmospheric forcings.

2 The investigated site

The measurements were performed at the distal end of the ice-covered section i.e. in the so-called Eispalast (hereafter abbreviated as EP). The name derives from a flat and homogeneous ice surface, which is located in a hall of ca. 50 m length and about 15 m height (Fig. 1). The frontal part of the hall is confined by two narrow, mostly ice-covered and elevated openings, whereas the distal section develops into a wide, down-sloping and ice-free gallery. EP itself covers an area of about 1000 m^2 and hosts an ice volume of ca. 3700 m^3. GPR measurements and several drillings revealed a maximum ice thickness of 7 m (Behm and Hausmann, 2007; May et al., 2010) and indicate that the ice body smoothly thins towards the margins similar to an asymmetric bowl. The ice thickness at the location of our investigation is 3.3 m and the surface itself slightly slopes towards the distal margin. During cave visits we rarely observed dripping water from the ceiling of the hall. In spring 2009, however, we noted enhanced seepage water emerging from an ice column in the rear section of EP (Fig. 1, background).

ERW is partly used as a show cave. Some disturbance of the natural ventilation regime may be expected due to the closure of a door at the main entrance during summer. Another influence may arise from visitors of the cave (also during summer). However, the measurement site is situated well beyond the visitor's path where temperature measurements do not indicate significant effects on the thermal regime at this location. Regarding air flow, the measurement site is situated in an area of divergence and ventilation is accordingly weak. Thus we are confident that potential disturbances are negligible in the context of this short-term study. Notably, the door is kept open during winter when the cave environment is truly undisturbed.

3 Measurements

The data were collected by a specifically designed automatic weather station measuring air temperature, humidity, wind speed and direction at two levels above the surface (1 and 4 m). Further, we measured air pressure, down- and upwelling long-wave radiation components and ice temperatures at 0.5 and 3.1 m below the ice surface. An ultrasonic ranger was installed to continuously monitor ice thickness changes. The data were stored onto a logger in 10 min intervals. Figure 1 shows the measurement site and the setup of the instruments.

The cave was visited nine times between May 2007 and October 2009 to maintain the sensors, to collect the data, and to perform supporting measurements and observations. At these occasions, the mass balance of the ice was also monitored by stake readings. We also refer to data from the analysis of an ice core retrieved in June 2007 (density and grain structure; May et al., 2010). Further observations concern e.g.

the surface conditions or the occurrence of seepage water. Attempts to measure the discharge of seepage water entering EP failed.

Meteorological measurements in cave environments are challenging for various reasons. This includes limited accessibility and according logistic efforts concerning e.g. power supply and keeping the instruments operative in moist conditions. Further, the natural variability of the relevant environmental parameters is low and close to the detection limit of standard sensors. On the other hand, cave measurements benefit e.g. from the lack of solar radiation which can not affect temperature or long-wave radiation sensors. We mostly used standard research components, but put essential effort into sensor calibration before and after field work. Notable experiences are that ultra-sonic sensors proved reliable for measuring the low wind speeds and the small surface height changes. On the other hand, an ice temperature sensor failed completely and the performance of the humidity and radiation sensors may have degraded by condensate or dust, which can hardly be quantified. More details about the sensors used are documented in Campbell (2001a, b) or Gill (2010) and will be discussed below (Sects. 5.2 and 5.4.1). Unfortunately, there was also a gap in the data due to an intermittent failure of the logger in May 2009. Therefore, this study is mostly limited to a reference period from December 2007 until November 2008.

4 The model

A one-dimensional numerical mass and energy balance model is used to simulate the seasonal evolution of the ice and its interaction with the atmosphere and the underlying rock (SNTHERM, Jordan, 1991). This model is adaptable to a wide range of environmental conditions and is widely used in snow and ice research (Rowe et al., 1995; Cline, 1997; Hardy et al., 1998; Gustaffsson et al., 2001; Olefs and Obleitner, 2007; Fox et al., 2008). The ice and rock substrates are described in terms of matrices (ice and dry solids) and void spaces (occupied by liquid water and moist air). The model calculates vertical profiles of the bulk physical parameters including temperature, density, grain size, and liquid water content by solving the governing equations of the processes determining heat, mass, and momentum exchange within control volumes. A full discussion of the associated parameterisations and numerical methods is given in Jordan (1991). Effects due to horizontal energy transfer are generally neglected.

Principally, the model solves the following energy balance equation:

$$\frac{dE}{dt} = \int_{z=0}^{H} \left(\frac{d}{dt} \left(c_p \rho(z) T(z) \right) \right) dz + \mathrm{LR_{MF}} = \mathrm{NR} + \mathrm{SHF} + \mathrm{LHF} + \mathrm{PHF} \tag{1}$$

The left-hand terms represent the rate of the subsurface changes of internal energy E due to associated changes in heat content and phase transitions within the control volume. Basically, this involves the processes of heat and vapour diffusion, liquid water transport, and latent heat exchanges due to melting and freezing. The right-hand terms represent the driving surface fluxes i.e. net radiation (NR), sensible heat flux (SHF), latent heat flux (LHF), and heat transfer due to precipitation (PHF). In a cave environment NR is confined to the long-wave components only and PHF considers the thermal effects related to seepage water. The surface fluxes are defined positive if providing mass and energy to a layer or the surface. The associated changes in mass M (determined by ice thickness H and density ρ) consider precipitation/seepage water (P), evaporation/condensation or sublimation/deposition (E/C) runoff or freeze (R_{MF}). The latter two terms provide a link to the energy balance:

$$\frac{dM}{dt} = \int_{z=0}^{H} \left(\frac{d}{dt} (\rho(z)) \right) dz \approx \rho \frac{dH}{dt} = P + E/C + R_{\mathrm{MF}}$$

The model domain is based on 1 m of rock upon which the physical and thermal development of the ice body is simulated in response to the atmospheric forcing. The initial ice thickness is 3.3 m corresponding to the measured depth of several drillings to the bed rock. The simulations consider 147 layers (rock and ice) and the resolution of the grid ranges between 1 and 0.001 m, the latter being specified at the material interfaces.

To initialize the simulations, vertical profiles of temperature, bulk density, liquid water content and grain size were prescribed throughout the vertical domain. The density profile is based on analysis of an ice core drilled in June 2007 (May et al., 2010) and the temperature profile is derived from the ice and rock temperature measurements. The latter were taken horizontally at the level of the ice surface, which may not be fully representative for the actual conditions at the bottom ice/rock interface.

The simulations are forced by meteorological data from the lower measurement level (1 m). This is based on a rough consideration of fetch criteria yielding 1–2 m as a critical level where the nearest local roughness changes may induce an internal boundary (Rao et al., 1974; Bradley, 1988). A corresponding sensitivity study proves that using data from the upper level does not critically change the flux calculations. This indirectly confirms that there was no significant vertical flux divergence. The simulations were started at a time with minimum vertical temperature gradients (December) to facilitate the spin-up of the model. The subsequent simulations were performed on an hourly basis and cover a full annual cycle (2008), which henceforth is considered as the reference period.

Some modifications of the model parameterisation were necessary to properly treat the specific conditions in a cave. Thus, the model was modified to treat rock (limestone) as a soil species with appropriate physical and thermal characteristics (density, thermal conductivity, water permeability). Heat conduction is parameterized according to Yen (1962) and parameterisation of the turbulent fluxes is based on Monin-Obukhov framework. Surface roughness length is specified as 0.001 m and stability effects are parameterized according to Högstrom (1988). Further modifications of the original model parameterization concern appropriate treatment of metamorphosis and water transport processes within the ice. The inherent uncertainties regarding model input and parameterisation will be considered in the context of sensitivity studies (Sect. 5.4).

5 Results and discussion

The following evaluation and discussion of the mass and energy balance of ice at EP is based on combining observational data and verified model output. We mainly consider a so-called reference run which is based on optimum data covering a full annual cycle (December 2007 until November 2008).

5.1 Local meteorological and glaciological conditions

The climatological conditions outside ERW are characterized by an average air temperature of 4.0 °C, an average precipitation of 1836 mm and a prevalence of north-westerly winds. These data refer to the nearest climate station located at a distance of 50 km to the north and at about the same elevation as the cave entrance (Feuerkogel 1618 m; ZAMG, 2010). Evaluation of long-term temperature measurements within the cave show a progressive attenuation of the outside temperature fluctuations towards the cave interior (Fig. 2). Thus, the average seasonal temperature variation at EP is only about 1.5 °C compared to 6 °C at the entrance and 17 °C in the outside atmosphere. These findings conform to the observations by Silvestru (1992), Thaler (2008) and Schöner et al. (2010).

The average conditions at the measurement site itself are characterized by an air temperature close to the melting point (–0.45 °C), relative humidity at saturation (99.7%) and low wind speeds (0.14 ms^{-1}). Figure 3 depicts more details in terms of monthly values at several measurement levels in the air and within the ice. Air temperatures can be as low as –1.5 °C during winter, while being slightly positive from May to October (+0.1 °C). The extreme values range between –1.8°C and +0.3°C. The air is significantly dryer during winter when wind speeds are higher (max. 0.6 ms^{-1}) and the direction of the air flow features a clear bimodal frequency distribution with prevailing outflow during summer and inflow during winter (Fig. 4). Note however that reversals in air flow occur quite frequently which is particularly pronounced during winter.

TCD
4, 1741–1779, 2010

This meteorological regime is rather typical for a dynamically ventilated cave system. Overall, the temperature, humidity and wind measurements reveal a distinct winter and summer regime terminating in May and November, respectively. This is corroborated by the seasonal pattern of the wind regime which advects cold air from outside during winter and cools the host rock to about −1.5 °C. Summer is characterized by a weak outflow of colder air from within the cave. Mean annual air temperature is slightly negative, thus just matching a basic condition for the existence of perennial ice. This subzero temperature regime is mainly supported by cooling due to unidirectional ventilation during winter and associated ice sublimation, as was found also elsewhere (Silvestru, 1999). Trapping of cold air can only play a very local and intermittent role in ERW. This is also due to frequently reversing air flow, which is particularly pronounced during winter. Investigations by Oedl (1923), Saar (1957), Thaler (2008) and Schöner et al. (2010) indicate that these events are associated with major synoptic events inducing a reversal of thermally induced pressure gradients.

The vertical profiles of air temperature and humidity are subject to a distinct seasonal variability, too. During summer, we observe inversion conditions and an associated increase of humidity with height above ice surface (Fig. 5). Ice temperatures are at or close to the melting point and slightly decrease with depth. This conforms to the usual conditions above a melting glacier surface (Obleitner, 2000). These gradients reverse sign during winter which is mainly attributed to advection of cold and dry air from outside the cave. At this time the deeper ice layers and the rock dome are warmer than the surface. This marked reversal of the vertical temperature and humidity gradients has important consequences for the energy balance of the ice.

The glaciological measurements reveal a loss of about 3.5 cm of ice during the reference period (Table 1). About 90% of this value was achieved during the melt period lasting from June until November. The remainder occurred during winter which is attributed to sublimation. There was no pronounced accumulation period observable during the reference period which will be further discussed in the subsequent sections.

TCD
4, 1741–1779, 2010

6 Model verification

The following investigation of the energy and mass budget of ice is strongly based on model output. Proper verification is therefore essential employing data not used as input for the simulations. Figure 6 demonstrates that the simulation captures the seasonal evolution of ice thickness, which in view of the constant density is considered as an appropriate measure of mass balance. The verifying sonic data are representative for a surface area of ~20 cm and have a nominal accuracy of 0.3 cm (Campbell, 2010b). Effective accuracy of the latter is certainly better due to the small temperature range in a cave environment. Stake measurements are more sensitive to subjective errors and the small-scale variability of the surface (Obleitner, 2000). Thus, the indicated increase of ice thickness in late summer 2008 is not interpreted as an accumulation event, but is attributed to a single disturbance of the stake environment imposing a systematic offset henceforth. As inherent shortcomings of the simulations we note that sublimation is underestimated, ablation starts too late, while the subsequent melt rate is overestimated. There was no straightforward improvement of simulations with these respects which required further investigation. In part, however, these deficiencies may be due to the limited grid resolution and the individual effects cancel each other out on a seasonal time scale.

Surface temperature is considered as a key parameter reflecting the skill of the model to simulate the processes determining the energy balance. Comparison with measured values reveals that the seasonal development of surface temperature is captured at RMSE=0.18 °C and r^2 =0.95 (Fig. 6, upper panel). The annual averages agree within 0.2 °C, which roughly corresponds to the effective accuracy of the associated long-wave radiation measurements (Obleitner and deWolde, 1999). The ice temperatures at 0.5 and 3 m below the surface are simulated with a similar skill (RMSE=0.06/0.15 °C; Fig. 6 lower panels). Note that the nominal accuracy of the used thermometers is specified as ±0.2 °C (Campbell, 2010b), which was improved by laboratory recalibrations ±. The overall noisy signal reflects the digitizing accuracy of the logger extension module measuring these sensors. The results further show a slight tendency to simulate too high values at the upper level and too low values at the lower level. In part this may be related to the inherent uncertainty in relating the exact position of the measurement levels to the model nodes.

7 Energy and mass balance

Table 1 points out the overall small magnitude of the calculated energy balance components compared to outside snow/ice environments (e.g. Greuell et al., 1997; Obleitner, 2000; Hock, 2005; Armstrong and Brun, 2008; Giesen et al., 2009;. This is essentially true for net radiation which in a cave environment is constricted to the long-wave components. Nevertheless, long-wave radiation constitutes the most significant source of energy for the surface. This is related to the overall higher temperature of the rock dome compared to the ice surface (Fig. 3).

On average the turbulent fluxes both withdraw energy from the ice surface, essentially during winter (Table 1). Heat fluxes at the lower boundary play an alternating role. Driven by molecular heat conduction in response to the associated temperature gradients, the basal rock withdraws some heat during summer, while providing energy during winter. Heat transfer by seepage water is negligibly small and not further considered. The annual net balance of these fluxes leaves energy to warm and melt the ice, which is corroborated by the observed decrease in ice thickness.

Figure 7 demonstrates the seasonal evolution of the energy balance in terms of monthly values. Net radiation is positive from April to November, which coincides with the period of positive rock temperatures (Fig. 3). Net radiation diminishes towards a minimum in March when successive cold events penetrates far into the cave and cool the rock surfaces to about $-1.5\,^{\circ}$C. The turbulent heat fluxes are positive from June to November, when air temperature and water vapour are higher than at the ice surface (Figs. 3 and 5). During winter the turbulent fluxes effectively withdraw energy from the surface which contributes to an associated cooling and loss of ice due to sublimation. Molecular conduction within the rock underneath the ice is a heat sink during summer, while warming the ice at its base during the cold season. In response to the net of these fluxes the ice experiences an energy deficit from December until March (Fig. 7, lower panel). However, this is overcompensated by excess energy during the period April until November which predetermines the positive sign of the annual energy balance.

The calculations also promote some consideration of the developments within the ice. Thus, Fig. 8 shows the evolution of ice temperature demonstrating that the system is strongly determined by the atmospheric at the surface. The cooling of the ice in winter is mainly associated with episodic cold waves which finally penetrate almost to the bottom of the ice. The warming phase during summer is of a more continuous nature and does not reach as far down. The associated surface melt water gradually soaks the top few centimetres of the ice and runs off finally. This is corroborated by visual evidence during the cave visits. Notably, neither observations nor simulations indicate basal melt of ice under current conditions.

Putting these results in a broader context, the investigations by Schöner et al. (2010) suggest that the basic constellation of the energy balance may be characteristic for the major ice-bearing part of ERW. In particular, this concerns the prevalence of sublimation during winter and condensation during summer. Fluxes have not been calculated, but the documented data suggest that the turbulent fluxes may be larger in the outer cave sections due to enhanced gradients and wind speeds. Further, there is evidence of a significantly larger variability of the annual mass balance of ice in the outer parts of ERW (±15 cm) compared to EP (2–4 cm). This may be related to a correspondingly larger variability of the meteorological regime, topographic effects (different slopes, different water sources) and some indicated human activities.

Evaluating historical photographs at EP, Spötl et al. (2008) document that 10–20 cm of ice was lost since the 1920s. This estimate refers to a location ca. 10 m west of our measurements site. However, this indicates that the currently observed retreat (2–3 cm yr^{-1}) is not fully representative on longer time scales. In particular there is evidence for more positive mass balances prior to about 1930 (May et al., 2010), which roughly conforms to evidences elsewhere in the Alps (Luetscher et al., 2005).

TCD
4, 1741–1779, 2010

F. Obleitner and Ch. Spötl

Ohata et al. (1994a, b) investigated the energy balance of perennial ice in a collapsed lava tube on Mt. Fuji (Japan). Its meteorological regime basically conforms to a dynamically ventilated cave though featuring topographically induced aspects of static caves as well. Transferring their numbers of the calculated energy balance and comparing them to our results reveals a comparable magnitude of the fluxes (NR=0.22, SHF= −0.17, LHF= −0.09 Wm^{-2}). The stronger radiation input can be explained by the higher ground temperatures (lower altitude and volcanic rock). We also note the prevalence of sublimation during winter, which thus may be a general characteristic of ice caves. Average ice thicknesses in the Fuji cave recently decreased at a rate of ca. 5 cm yr^{-1} (1989 until 1992), which is larger than observed at EP. However, the authors note a considerable variability towards the outer cave sections, which conforms to the observations in ERW.

Luetscher et al. (2008) investigated the energy and mass balance of perennial ice in Monlesi cave (Switzerland). This cave experiences similar outside temperatures as ERW and due to its sag-like topography there is a weak oscillating air flow during summer and unidirectional ventilation during winter. Referring to the documented data during a year with a negative mass balance (−10 cm during 2002–2003), a straightforward comparison of the energy balance components is partly hampered because of different approaches. Thus we can only consider the sum of radiative and conductive fluxes (including side walls) yielding larger values than calculated for EP (4.4 vs. 1.1 Wm^{-2}). The turbulent fluxes can be transferred more straightforwardly yielding higher values, too (−1.5 /−1.13 vs. −0.16/−0.17 Wm^{-2}). Seemingly this is mainly due to the assumption of higher wind speeds (not measured). Accumulation in Monlesi cave is controlled by deposition of seasonal snow and percolating water. The former does not play a role in ERW, while it is a common feature that seepage water predetermines the interannual variability of the mass balance.

TCD
4, 1741–1779, 2010

F. Obleitner and Ch. Spötl

7.1 Sensitivity studies

A set of additional simulations was performed by systematically changing individual model input parameters. This kind of studies proved valuable to judge the potential influence of uncertainties regarding model input and parameterization (Obleitner and Lehning, 2004). Moreover, the potential response of the mass balance on assumed environmental (climate) changes can be addressed as well (Oerlemans and Reichert, 2000). Generally, the usually large uncertainties associated with albedo, turbulent fluxes or metamorphosis do not play a role in the context of cave ice simulations.

7.1.1 Effects due to uncertainties of the input data

Air temperature was measured with an accuracy of ±0.1 °C. Table 2 shows that this induces significant effects on net radiation and the turbulent fluxes compared to the reference run. A positive deviation reduces calculated net radiation, which via surface temperature is overcompensated by a smaller energy deficit by the turbulent heat fluxes (Table 2b). The net gain in energy yields enhanced melt and about 5 mm of ice are lost additionally. Applying the same uncertainty as a cooling saves 4 mm of ice compared to the reference run (Table 2c). Introducing a 1% uncertainty in measured humidity mainly affects the latent heat exchange, but the net effect on the calculated mass balance is small due to the compensating response of net radiation and sensible heat flux (Table 2d). Changes in wind speed within the measurement accuracy lead to a slightly enhanced mass loss (Table 2e). Note that the indicated uncertainties correspond to the nominal accuracies of the used sensors (Gill, 2010), while their effective accuracy was certainly better due to recalibration efforts. Long-wave radiation was measured to within ±0.5 $\mathrm{W m^{-2}}$ (Obleitner and deWolde, 1999). Porting this uncertainty into the simulation has a strong impact on the results and almost doubles calculated melt (Table 2f). Consideration of changes in parameterisation of the turbulent fluxes (roughness parameter set to 0.01 m instead of 0.001 m) did not show significant effects on the results (Table 2g). This is mainly attributed to the overall small magnitude of

TCD
4, 1741–1779, 2010
Mass and energy balance of ice
F. Obleitner and Ch. Spötl

the fluxes due to the low wind speeds and the small gradients of the driving variables, respectively.

Some input data could not be measured appropriately. To optimize the reference run with respect to the effect of seepage water, an amount of 0.001 mm h^{-1} (Table 2d) was prescribed whenever the host rock temperature was positive and surface temperature was negative. The latter constraints were considered to represent conditions when seepage water is principally available and can refreeze on the still cold ice surface. A corresponding sensitivity study shows that this saves about 3 mm (Table 2h). Furthermore, there is an uncertainty regarding the input of the vertical temperature and density profiles at the start of the simulations. As documented above this was based on ice temperature measurements at two depths only and the rock temperature was derived from near-surface, horizontally aligned borehole measurements and not at the bottom as required. Density was derived from ice core analysis and bears an uncertainty in the order of 10% (May et al., 2010). The potential effects of these uncertainties on the simulated energy and mass budget are insignificant as was checked by corresponding sensitivity studies.

Overall, the sign and magnitude of the calculated fluxes proved robust with respect to best estimated measurement or parameterisation uncertainties. Judging by a 10% deviation compared to the reference run, the calculated mass balance is most sensitive with respect to proper treatment of long-wave radiation, air temperature and input of seepage water. This emphasizes that cave measurements require special effort regarding the choice of corresponding instruments.

7.1.2 Potential climate impacts

Sensitivity studies may also serve to investigate the energy and mass balance in response to potential changes in the environmental conditions. In this context, however, we do not refer to regional climate scenarios as e.g. put forward by Zhao (2007). Instead, we focus on a few extremes which are depicted in Table 2. Thus, we firstly consider a meteorological setting where air temperature remains positive throughout

TCD
4, 1741–1779, 2010

the year. An equivalent increase in air temperature (+1.5 °C, see also Fig. 3) yields an outstanding loss of ice (10 cm yr^{-1}, Table 2i). The reversed sign of GHF indicates that in this case there would be some melt at the rock/ice interface, too. The opposed assumption of a 0.5 °C decrease in annual temperature represents a regime where significant melt could not occur any more (Fig. 3). Corresponding simulations indicate that under such conditions there would still be a decrease in ice thickness (2 cm yr^{-1}) due to enhanced and continuous sublimation (Table 2j).

Exemplifying the potential of natural feedback processes, we recall that an increase in outside air temperature will also change the rock dome temperature and correspondingly emitted long-wave radiation. The associated sensitivity study demonstrates that this positive feedback yields an enhanced effect compared to single parameter changes (Table 2k).

We further consider the sensitivity of the calculated annual mass balance of the ice at EP in response to monthly changes in temperature and input of seepage water. Increasing the temperature of individual months by 1 °C has mainly effects during the melt season and results in more negative annual mass balances compared to the reference run (Fig. 9). This is due to enhanced energy input and a correspondingly longer melt period. The small saving effects during winter are due to less efficient sublimation. Refreezing seepage water generate less negative mass balances. To realistically constrain the inherent effects we firstly recall the relevant environmental conditions. These are characterized by a precipitation maximum in June and a snow melt run-off maximum in May/June (ZAMG, 2010). Further, the percolation of meteoric water into the cave requires the existence of open conduits which can only occur at positive rock temperatures. To roughly account for these constraints, the respective sensitivity study considers input of seepage water only during periods when the measured rock dome temperature is positive and the ice surface temperature is negative. The results indicate that seepage water has a major mass saving effect during spring and to a minor extent in autumn (Fig. 9).

A further study aimed at encompassing environmental conditions that prohibit any loss of ice. It was already shown that this cannot be achieved by just reducing annual air temperatures (Table 2j). This is due to ongoing sublimation which must be compensated by considerable input of seepage water that refreezes whenever the surface temperature is negative (0.05 mm h^{-1}, Table 2l).

7.1.3 Potential effects of the cave management

ERW is subject to some cave management activities including closure of the entrance door during summer (May until October). The aim of this action is to prohibit the natural outflow of cold air during summer, which is thought to protect the ice. The actual effect, however, is difficult to quantify due to the lack of corresponding data or simulations of the air circulation within the cave. For the purpose of a corresponding study we assume that opening of the door during summer may increase air temperature by 0.1 °C and increase wind speeds by 0.1 ms^{-1}. The simulation results indicate that closing the door could thus save ca. 5 mm yr^{-1} of ice (Table 2m). However this is like overestimating the actual effect, because there is a secondary entrance which is not closed and provides natural ventilation all the year round.

Cave management may also involve changes of local water supply, which is not documented regarding the EP investigation site itself. However, we note a regular increase in measured ice thickness during November, which is hard to understand because meteoric precipitation is minimal at that time of the year (dashed lines in Fig. 10). This likely anthropogenic measure, however, does not seriously affect the overall suitability of the measurement site or the results of this study and was not further investigated. However, Schöner et al. (2010) indicate that water management may well affect the ice development in outer parts of ERW.

TCD
4, 1741–1779, 2010

F. Obleitner and Ch. Spötl

8 Temporal and spatial representativity

The representativeness of the reference year 2008 may firstly be judged by climate data measured in the ERW environment. Relevant data (ZAMG, 2010) reveal that the years 2008 and 2009 were among the warmest during the last decade, the latter year being slightly colder (4.4 °C vs. 4.2 °C compared to the long-term average 3.6 °C). There was less precipitation during the colder year 2008 (2248 vs. 1777 mm), which experienced more days with a closed snow pack on the other hand (202 vs. 182 days).

;ig. 10 documents the evolution of mass balance for an extended period considering all available measurements (June 2007 until September 2009). This series covers the reference run (year 2008, dashed lines in Fig. 10), but is interrupted during spring 2009 due to intermittent logger failure. Nevertheless, the data reveal a considerable variability of the mass balance components within the two subsequent years. This is less pronounced regarding ablation (3.9 cm vs. 3.2 cm) while accumulation strikingly differs (negligible during spring 2008 vs. 7.3 cm during spring 2009). This is confirmed by independent data (stake and sonic ranger) and the evidence points towards a different availability of refreezing seepage water during the two years. This reasoning is corroborated by observations of an ice column in the neighborhood of the measurement site (Fig. 1, background). Compared to the year before, an associated water conduit provided unusual amounts of water during spring 2009. This water gradually spread over the rear parts of EP, thereby refreezing at the measurement site, too. The latter was supported by an enhanced cold content of the ice due to lower temperatures during the preceding winter.

These findings are supported by corresponding model studies. Recall that a negligible input of seepage water is necessary to reproduce the measured mass balance in 2008 (reference run). As expected, the development during 2009 cannot be reproduced by a simulation without considerable input of seepage water in spring 2009. Forcing the model accordingly (0.3 mm h^{-1} of seepage water in May; 0.03 mm h^{-1} in June) indeed captures the observed development. These findings are relevant for the interpretation of an ice core recovered in the front part of EP (Spötl, 2008; May et al., 2010). Note however, that due to the adverse surface slope the drilling site is certainly less affected by seepage water from the mentioned ice column.

9 Summary

This work was performed within a multidisciplinary project focussing on glaciological and meteorological aspects related to perennial cave ice. The specific focus is on a process-oriented assessment of the energy and mass balance of the ice employing measurements and numerical modelling.

Year-round measurements have been performed in a dome shaped and ice covered section of Eisriesenwelt cave (Austria) ca. 700 m behind the entrance. The measurement concept was designed to capture the vertical profiles of temperature (air, ice, rock), humidity and wind speed, as well as the long-wave radiation components and surface height changes. The site was visited nine times during the measurement period (2008–2009). Thereof we mostly consider a reference period covering a full annual cycle with optimum data.

The meteorological data conform to the basic characteristics of a dynamically ventilated cave system. Compared to the outside atmospheric conditions, there is an overall small seasonal and interannual variability of air temperature, humidity and wind speed. However, there is a distinct winter and summer regime. During winter there is a relatively strong inflow of cold air which by March cools the rock to subzero temperatures. During summer we observe slightly positive air temperatures and weak outflow from the cave interior. The mean annual air temperature is $-0.45\,^{\circ}$C, thereby just matching a basic condition for the existence of perennial ice. This subzero temperature regime is mainly supported by unidirectional ventilation during winter, while trapping of cold air plays only a very local and intermittent role. This is also due to frequent reversals of air flow which is particularly pronounced during winter and related to major synoptic events.

TCD
4, 1741–1779, 2010

The vertical profiles of air temperature and humidity are subject to a distinct seasonal variability, too. During summer, we observed inversion conditions and an increase of humidity with height above ice surface. During winter, these gradients reversed sign which is mainly an effect of advection of cold and dry air from outside.

There was a negative mass balance of the ice at the measurement site ($-3.5\,\mathrm{cm\,yr^{-1}}$) which is corroborated by independent measurements and the simulations. About 10% of this deficit is due to sublimation during winter, while the major loss resulted from melt during summer (May until November). Small amounts of accumulation occurred during spring due to refreezing seepage water.

Evaluation of the energy balance was based on employing a one-dimensional numerical model. The calculated energy balance of the ice is largely predetermined by input of long-wave radiation originating at the host rock surface. On average the turbulent fluxes withdraw energy from the surface. This is more pronounced during winter due to enhanced circulation and lower humidity. During summer the turbulent fluxes provide some negligibly small amounts of energy, which enhance melt. Basal heat exchange at the rock/ice interface withdraws some heat during summer, while providing energy at the bottom of the ice during winter. The simulations also show that the thermal regime within the ice is strongly affected by multiple cold waves during winter, which progressively cool beyond the ice-rock interface. The summer heat wave does not reach that far down. These findings are notable with respect to the existence of ice under current conditions.

Model sensitivity studies prove the reliability of these results regarding diverse measurement uncertainties. Mean monthly sensitivity characteristics indicate that the annual mass balance strongly depends on late summer temperatures and the availability of seepage water in spring. The latter also induces a considerable temporal and spatial variability, which is confirmed by the investigation of the development during successive years with significantly different mass balances.

Therefore, future studies may be directed right towards the latter topic. This may include development of proper in-situ measurement techniques as well as employing e.g. tracer methods. There is also a basic interest in developing long-term monitoring concepts to be transferred to other caves, too. To start with, thermistor strings were installed at EP, aiming at long-term measurements of the vertical profiles in the air, as well as within the ice and the host rock, respectively. These investigations are supported by mass balance measurements using stakes.

Accompanying investigations indicate that the investigated site is not fully representative of the ice bodies closer to the entrance of Eisriesenwelt. This issue needs further investigation based on new observations and/or modelling including numerical simulation of the air flow within the cave. The latter is an overall open and challenging topic fostering a process-oriented understanding of e.g. cave ice chemistry or investigation of the response of ice in other caves and on longer time scales.

Acknowledgements. This work was funded by the Austrian Academy of Sciences (project AUSTRO*ICE*CAVES*2100) and Innsbruck University. Development of instrumentation was supported by Kroneis GmbH. and Sensalpin GmbH. Access to the cave and logistic support was generously provided by Eisriesenwelt GmbH and field work was assisted by several students of the Institute of Meteorology and Geophysics, Innsbruck University.

References

Armstrong, L. and Brun, E. (eds.): Snow and climate: Physical Processes, Surface Energy Exchange and Modeling, Cambridge University Press, 254 pp., 2008.

Balch, E. S.: Glaciers or freezing caverns, Philadelphia, Allen, Lane & Scott, reprinted 1970 by Johnson Reprint Corp., NY, USA, 338 pp., 1900.

Behm, M. and Hausmann, H.: Eisdickenmessungen in alpinen Höhlen mit Georadar, Die Höhle, 58, 3–11, 2007.

Bradley, E. F.: A micrometeorological study of velocity profiles and surface drag in the region modified by change in surface roughness, Q. J. Roy. Meteorol. Soc., 94, 361–379, 1988.

Campbell: Instruction Manual, Model 107 Temperature Probe, Campbell Scientific, Inc., available at: http://www.campbellsci.com/documents/manuals/107.pdf, 2010a.

Campbell: Instruction Manual, SR50A Sonic Ranging Sensor, Campbell Scientific, Inc., available at: http://www.campbellsci.com/documents/manuals/sr50a.pdf, 2010b.

Canaval, R.: Ein Eiskeller in den Karawanken, Carinthia, II, 83, 178–180, 1893.
Citterio, M., Turri, S., Bini, A., and Maggi, V.: Observed trends in the chemical composition. δ18O and crystal sizes vs. depth in the first ice core from the LoLc 1650 "Abisso sul margine dell'Alto Bregai" ice cave (Lecco, Italy), Theoretical and Applied Karstology, 17, 45–50, 2004.
Cline, D. W.: Snow surface energy exchanges and snowmelt at a continental midlatitude Alpine site, Water Resour. Res., 33(4), 689–701, 1997.
de Freitas, C. and Littlejohn, R.: Cave climate: Assessment of heat and moisture exchange, Int. J. Climatol., 7, 553–569, doi:10.1002/joc.3370070604, 1987.
Erhard, Ch. and Spötl, C.: Karst geology and cave fauna of Austria: a concise review, Int. J. Speleol., 39, 71–90, 2010.
Ford, D. and Williams, P.: Karst Geomorphology and Hydrology, London, Chapman and Hall, 601 pp., 1989.
Fox, A., Willis, I., and Arnold, N.: Modification and testing of a one-dimensional energy and mass balance model for supraglacial snowpacks, Hydrol. Proc., 22, 3194–3209, 2008.
Giesen, R. H., Andreassen, L. M., van den Broeke, M. R., and Oerlemans, J.: Comparison of the meteorology and surface energy balance at Storbreen and Midtdalsbreen, two glaciers in southern Norway, The Cryosphere, 3, 57–74, doi:10.5194/tc-3-57-2009, 2009.
Gill: MetPak II^{TM} Weather Station, a Gill Instruments Ltd., available at: http://www.gill.co.uk/data/datasheets/MetPakIIWebDatasheet.pdf, 2010.
Gressel, W.: Zur Dynamik in alpinen Höhlen, Die Höhle, 6, 67–71, 1955.
Greuell, W., Knap, W. H., and Smeets, P. C.: Elevational changes in meteorological variables along a midlatitude glacier during summer, J. Geophys. Res., 102(D22), 25941–25954, 1997.
Gustafsson, D., Staehli, W., and Jansson, P.: The surface energy balance of a snow cover: comparing measurements to two different simulation models, Theor. Appl. Climatol., 70, 81–96, 2001.
Hardy, J. P., Davis, R., Jordan, R., Ni, W., and Woodcock, C. E.: Snow ablation modelling in a mature aspen stand of the boreal forest, Hydrol. Process., 12, 1763–1778, 1998.
Hauser, E. and Oedl, R.: Die große Eishöhle im Tennengebirge (Salzburg, Eisriesenwelt), V. Eisbildungen und meteorologische Beobachtungen, Speläologische Monogr., Wien, 6, 77–105, 1923.
Hausmann, H. and Behm, M.: Application of ground penetrating radar (GPR) in alpine ice caves, The Cryosphere, submitted, 2010.

TCD
4, 1741–1779, 2010
Mass and energy balance of ice
F. Obleitner and Ch. Spötl

Hock, R.: Glacier melt: a review of processes and their modelling, Progress in Physical Geography, 29(3), 362–391, 2005.
Högström, U.: Non-dimensional wind and temperature profiles in the atmospheric surface layer: a re-evaluation, Bound.-Lay. Meteorol., 42, 55–78, 1988.
Holmlund, P., Onac, B., Hansson, M., Holmgren, K., Mörth, M., Ymani, M., and Persoiu, A.: Assessing the paleoclimate potential of cave glaciers: the example of the Scarisoara Ice Cave (Romania), Geogr. Ann. A., 87A, 193–201, 2005.
Jordan, R.: A one-dimensional temperature model for a snow cover: technical documentation for SNTHERM.89, CRREL, Spec. Rep. 91–16, 49 pp., 1991.
Kern, Z., Molnár, M., Svingor, E., Pers, A., and Nagy, B.: High-resolution, well-preserved tritium record in the ice of Bortig Ice Cave, Bihor Mountains, Romania, Holocene 19, 729–736, 2009.
Klappacher, W. and Haseke-Knapczyk, H.: Salzburger Höhlenbuch, 4, Landesverein für Höhlenkunde in Salzburg, 556 pp., 1985.
Lemke, P., Ren, J., Alley, R. B., Allison, I., Carrasco, J., Flato, G., Fujii, Y., Kaser, G., Mote, P., Thomas, R. H., and Zhang, T.: Observations: Changes in Snow, Ice and Frozen Ground, in: Climate Change 2007: The Physical Science Basis. Contribution of Working Group I to the Fourth Assessment Report of the Intergovernmental Panel on Climate Change, edited by: Solomon, S., Qin, D., Manning, M., Chen, Z., Marquis, M., Averyt, K. B., Tignor, M., and Miller, H. L., Cambridge University Press, Cambridge, United Kingdom and New York, NY, USA, 384 pp., 2007.
Luetscher, M. and Jeannin, P.: A process based classification of alpine ice caves, Theor. Appl. Karstology, 17, 5–10, 2004.
Luetscher, M., Jeannin, P., and Haeberli, W.: Ice caves as an indicator of winter climate evolution: A case study from the Jura Mountains, Holocene, 15, 982–993, doi:10.1191/0959683605h1872ra, 2005.
Luetscher, M., Bolius, D., Schwikowski, M., Schotterer, U., and Smart, P.: Comparison of techniques for dating of subsurface ice from Monlesi ice cave, Switzerland, J. Glaciol., 53(182), 374–384, 2007.
Luetscher, M., Lismonde, B., and Jeannin, P. Y.: Heat exchanges in the heterothermic zone of a karst system: Monlesi cave, Swiss Jura Mountains, J. Geophys. Res., 113, F02025, doi:10.1029/2007JF000892, 2008.
Mais, K.: Untersuchungen des Höhlenklimas in der Dachstein-Rieseneishöhle von 1910–1962,

TCD
4, 1741–1779, 2010

Mass and energy balance of ice

F. Obleitner and Ch. Spötl

Die Höhle, 50, 118–140, 1999.
Marshall, P. and Brown, M. C.: Ice in Coulthard Cave, Alberta, Can. J. Earth Sci., 11, 510–518, 1974.
May, B., Wagenbach, D., Spötl, Ch., Dublyansky, Y., and Liebl, J.: First investigations of an ice core from Eisriesenwelt cave (Austria), The Cryosphere, submitted, 2010.
Morton, F.: Die Eislöcher bei Eppan, Natur und Land, 48, 46 pp., 1962.
Nderichuk, V. and Dorofeev, E.: The influence of natural and anthropogenous factors on temperature regime and ice formations of Kungur Cave (Russia), Theor. Appl. Karstology, 7, 149–153, 1994.
Obleitner, F. and deWolde, J.: On intercomparison of instruments used within the Vatnajökull glacio-meteorological experiment, Iceland, Bound.-Lay. Meteorol., 92, 27–37, 1999.
Obleitner, F.: The energy balance of snow and ice at Breidamerkurjökull, Vatnajökull, Iceland, Bound.-Lay. Meteorol., 97, 385–410, 2000.
Obleitner, F. and Lehning, M.: Measurement and simulation of snow and superimposed ice at the Kongsvegen glacier, Svalbard (Spitzbergen), J. Geophys. Res., 19, D04106, doi:10.1029/2003JD003945, 1-12, 2004.
Obleitner, F., Thaler, K., Spötl, Ch., and Oedl, F.: Glacio-meteorological investigations in an Alpine ice cave (Eisriesenwelt, Austria), Geophysical Research Abstracts, Vol. 11, EGU2009-5875, 2009, EGU General Assembly, 2009.
Oedl, R.: Über Höhlenmeteorologie mit besonderer Rücksicht auf die große Eishöhle im Tennengebirge, Meteorol. Z., 40, 33–37, 1923.
Oerlemans, J. and Reichert, B.: Relating glacier mass balance to meteorological data by using a seasonal sensitivity characteristic, J. Glaciol., 46, 1521–1526, 2000.
Ohata, T., Furukawa, T., and Higuchi, K.: Glacioclimatological study of perennial ice in the Fuji Ice Cave, Japan, Part 1, Seasonal variation and mechanism of maintenance, Arctic Alpine Res., 26, 227–237, 1994a.
Ohata, T., Furukawa, T., and Higuchi, K.: Glacioclimatological study of perennial ice in the Fuji Ice Cave, Japan, Part 2, Interannual variation and relation to climate, Arctic Alpine Res., 26, 238–244, 1994b.
Olefs, M. and Obleitner, F.: Numerical simulations on artificial reduction of snow and ice ablation, Water Resour. Res., 43, W06405, doi:10.1029/2006WR005065, 2007.
Pavuza, R. and Mais, K.: Aktuelle höhlenklimatische Aspekte der Dachstein-Rieseneishöhle, Die Höhle, 50, 126–140, 1999.

TCD
4, 1741–1779, 2010

Mass and energy balance of ice

F. Obleitner and Ch. Spötl

Rao, K., Wyngaard, J., and Coté, O.: The structure of the two-dimensional internal boundary layer over a sudden change of surface roughness, J. Atmos. Sci., 31, 738–746, 1974.
Rowe, C. M., Kuiven, K. C., and Jordan, R.: Simulation of summer snowmelt on the Greenland ice sheet using a one-dimensional model, J. Geophys. Res., 100, 16265–16273, 1995.
Saar, R.: Eishöhlen, ein meteorologisch-geophysikalisches Phänomen, Untersuchungen an der Rieseneishöhle (R.E.H.) im Dachstein, Oberösterreich, Geogr. Ann. A., 38, 1–63, 1956.
Saar, R.: Zur Frage des Einflusses der Grosswetterlage auf die Dynamik der Wetterhöhlen, Die Höhle, 8, 33–44, 1957.
Schöner, W., Weyss, G., and Mursch-Radlgruber, E.: Linkage of cave-ice changes to weather patterns inside and outside the cave Eisriesenwelt (Tennengebirge, Austria), The Cryosphere, submitted, 2010.
Silvestru, E.: Ultrasonic investigations on the underground fossil glacier in the cave Ghearul de la Scrioara (Romania), Trav. Inst. Spéléo. E. Racovitza, 31, 151–154, 1992.
Silvestru, E.: Perennial ice in caves in temperate climate and its significance, Theor. Appl. Karstol., 11–12, 83–94, 1999.
Spötl, Ch., Wagenbach, D., Obleitner, F., May, B., Behm, M., Schöner, W., Hausmann, H., Pavuza, R., Thaler, K., and Schöner M.: AUSTRO_ICE_CAVES-2010, Final project report, 51 pp., 2008.
Spötl, Ch.: Kryogene Karbonate im Höhleneis der Eisriesenwelt, Die Höhle, 59, 26–36, 2008.
Stoffel, M., Luetscher, M., Bollschweiler, M., and Schlatter, F.: Evidence of NAO control on subsurface ice accumulation in a 1200-yr old cave-ice sequence, St. Livres ice cave, Switzerland, Quaternary Res., 72, 16–26, 2009.
Thaler, K.: Analyse der Temperaturverhältnisse in der Eisriesenwelt-Höhle im Tennengebirge anhand einer 12-jährigen Messreihe, diploma thesis, University of Innsbruck, 93 pp., 2008.
Trimmel, H.: Gedanken über den Zusammenhang zwischen Höhleneis und Vegetationsbedeckung über einer Eishöhle, Die Höhle, 20, 4–8, 1969.
Wigley, T. and Brown, M.: The glaciers of caves: in The Science of Speleology, edited by: Ford, T. and Cullingford, C., London, Academic Press, 319–358, 1976.
Yen, Y.: Effective thermal conductivity of ventilated snow, J. Geophys. Res., 67, 1091–1098, 1962.
ZAMG: Central Institute for Meteorology and Geodynamics, Annals 2008, available at: http://www.zamg.ac.at/?x/klima/jb2008/index.html, 2010.
Zhao, C.: Global Climate Projections. In: Climate Change 2007: The Physical Science Basis.

Contribution of Working Group I to the Fourth Assessment Report of the Intergovernmental Panel on Climate Change, edited by: Solomon, S., Qin, D., Manning, M., Chen, Z., Marquis, M., Averyt, K. B., Tignor, M., and Miller, H. L., Cambridge University Press, Cambridge, United Kingdom and New York, NY, USA, 2007.

Table 1. Mean meteorological parameters and energy balance components. (winter: 1 December 2007–30 May 2008, summer 1June 2008–30 November 2008).

	year	winter	summer
air temperature	−0.44	−1.07	0.01 °C
rel. humidity	99.7	99.4	99.9 %
wind speed	0.14	0.21	0.09 ms^{-1}
net radiation	+1.00	+0.47	+1.53 Wm^{-2}
sensible heat	−0.16	−0.36	+0.04 Wm^{-2}
latent heat	−0.17	−0.35	+0.02 Wm^{-2}
energy change within rock	+0.07	+0.25	−0.12 Wm^{-2}
energy change within ice	+0.74	−0.08	+1.47 Wm^{-2}
ice thickness change	−0.034	−0.002	−0.032 m

Discussion Paper | Discussion Paper | Discussion Paper | Discussion Paper |

TCD

4, 1741–1779, 2010

Mass and energy balance of ice

F. Obleitner and Ch. Spötl

Table 2. Mean energy balance components (Wm^{-2}) for different model settings and resulting changes in ice thickness H (m). For abbreviations and key descriptions refer to the text.

		NR	SHF	LHF	GHF	dE/dt	dH/dt
a)	reference	1.00	−0.16	−0.17	0.07	0.74	−0.034
b)	$t+0.1$	0.91	−0.09	−0.12	0.06	0.76	−0.039
c)	$t-0.1$	1.10	−0.24	−0.23	0.08	0.71	−0.030
d)	$rh-1$	1.04	−0.14	−0.26	0.07	0.70	−0.033
e)	$ws+0.1$	1.02	−0.18	−0.17	0.07	0.74	−0.035
f)	$lw+0.5$	1.37	−0.20	−0.21	0.05	1.00	−0.063
g)	$z0=0.01$ m	1.02	−0.17	−0.18	0.07	0.74	−0.035
h)	without seepage water	0.98	−0.16	−0.17	0.06	0.70	−0.037
i)	$t+1.5$	0.37	0.64	0.31	−0.01	1.31	−0.111
j)	$t-0.5$	1.61	−0.68	−0.63	0.14	0.43	−0.010
k)	$t+0.1$ & $lw+0.50$	1.28	−0.13	−0.16	0.04	1.03	−0.070
l)	$mb=0\ 0$	1.00	−0.17	−0.17	0.07	0.72	+0.001
m)	$t+0.1$ & $ws+0.1$	0.98	−0.13	−0.15	0.06	0.76	−0.039

Discussion Paper | Discussion Paper | Discussion Paper | Discussion Paper |

TCD

4, 1741–1779, 2010

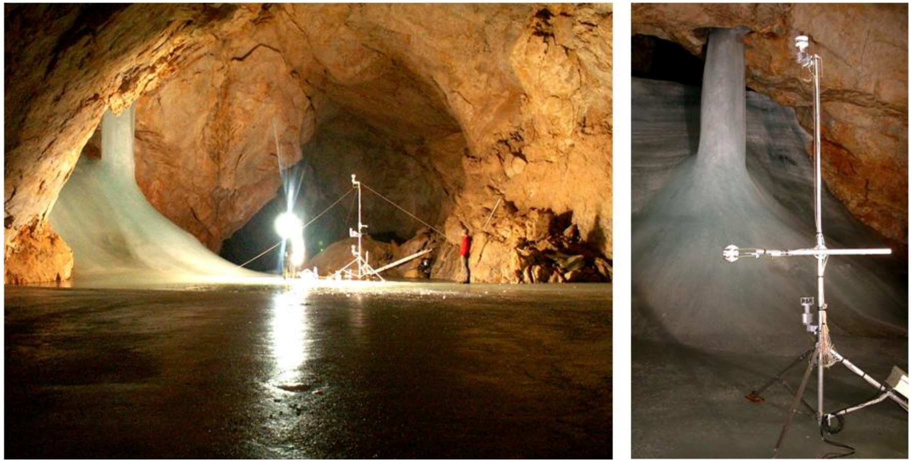

Fig. 1. View on the Eispalast measurement site (left) and on the meteorological instruments (right).

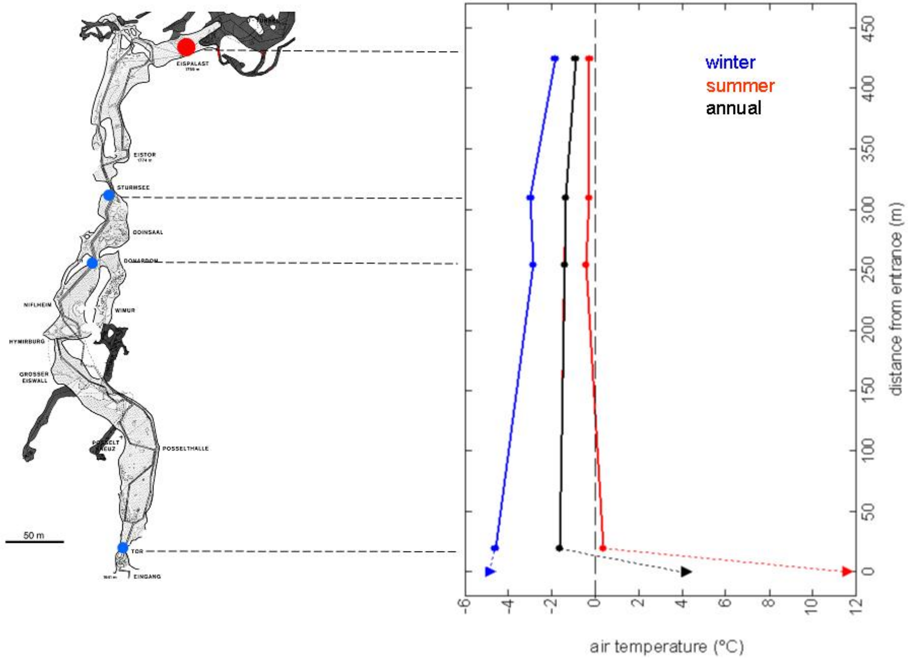

Fig. 2. Plan view of the ice bearing part of Eisriesenwelt (left) and seasonal average temperatures along this transect (1 December 2006 until 30 November 2007). Dots denoting long-term temperature measurement sites within the cave, triangles denoting air temperature outside the cave (Feuerkogel, 1618 m).

TCD
4, 1741–1779, 2010

Title Page
Abstract | Introduction
Conclusions | References
Tables | Figures
◀| |▶
◀ ▶
Back | Close
Full Screen / Esc
Printer-friendly Version
Interactive Discussion

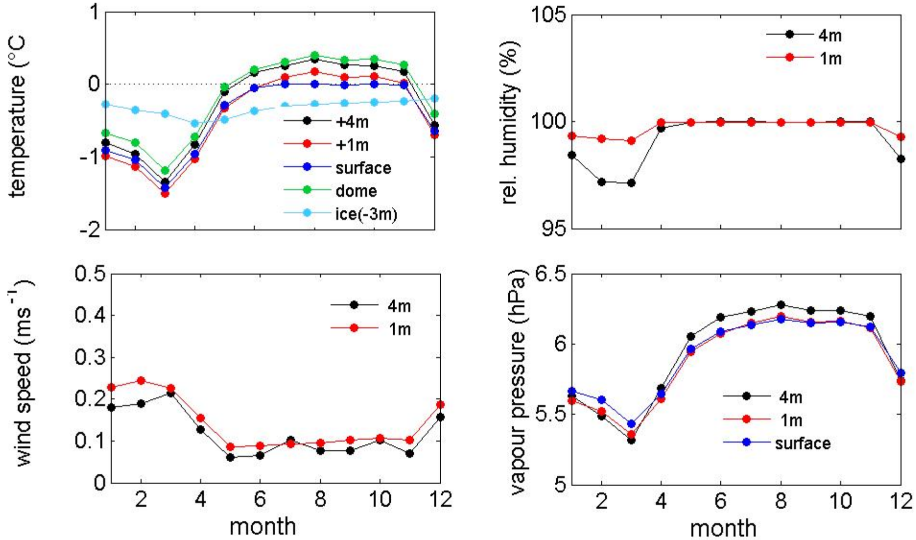

Fig. 3. Mean monthly values of measured temperatures (air, ice, rock) and humidity (upper panels) as well as of wind speed and vapour pressure (lower panels) at the EP measurement site.

TCD
4, 1741–1779, 2010

Mass and energy balance of ice

F. Obleitner and Ch. Spötl

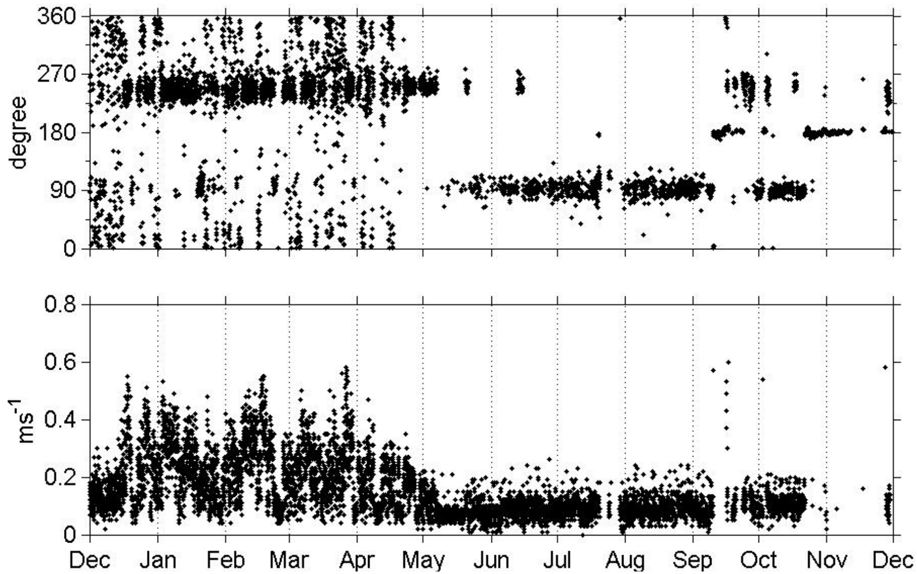

Fig. 4. Evolution of direction (upper panel) and velocitiy (lower panel) of the air flow at the measurements site. Inflow corresponds to westerly directions, outflow to easterlies.

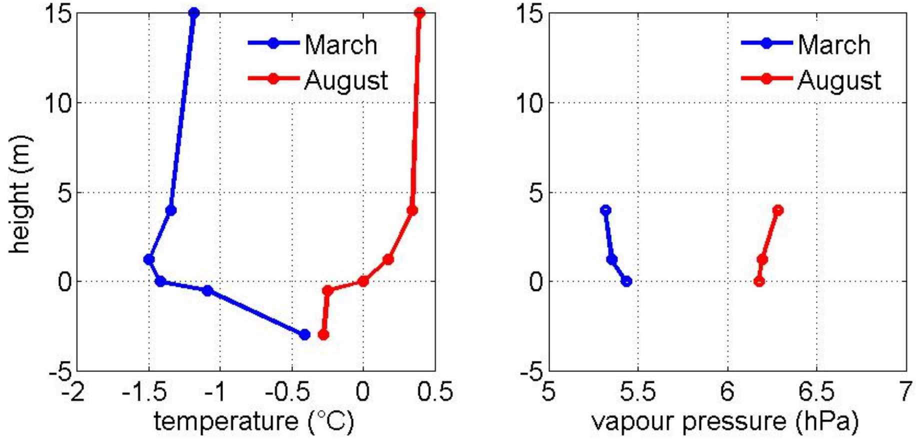

Fig. 5. Mean vertical profiles of temperature (air, ice, rock; left) and vapour pressure (right) measured at the EP measurement site during the warmest and coldest moth of the year.

TCD
4, 1741–1779, 2010

Mass and energy balance of ice

F. Obleitner and Ch. Spötl

Title Page
Abstract Introduction
Conclusions References
Tables Figures
Back Close
Full Screen / Esc
Printer-friendly Version
Interactive Discussion

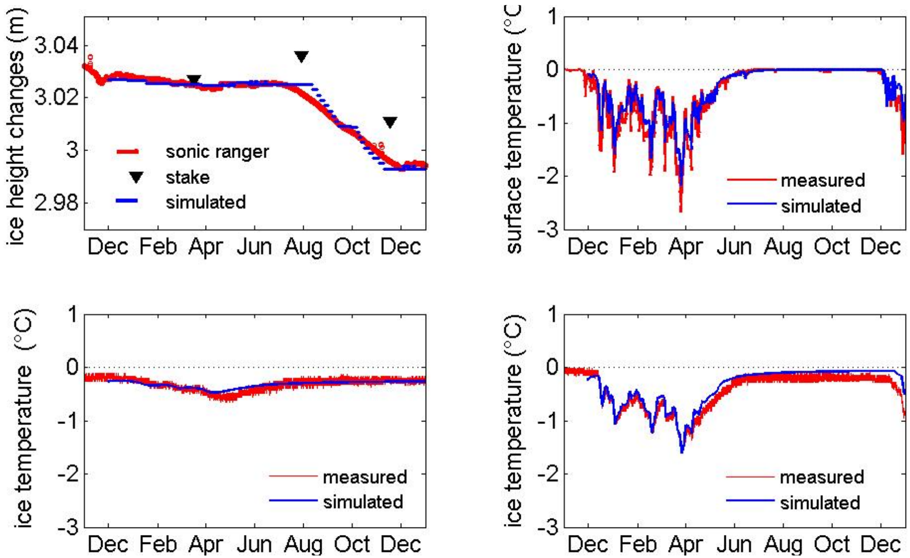

Fig. 6. The development of changes in ice thickness and surface temperature (upper panels) and of ice temperatures 3 m and 0.5 m below the ice surface (lower panels).

TCD
4, 1741–1779, 2010

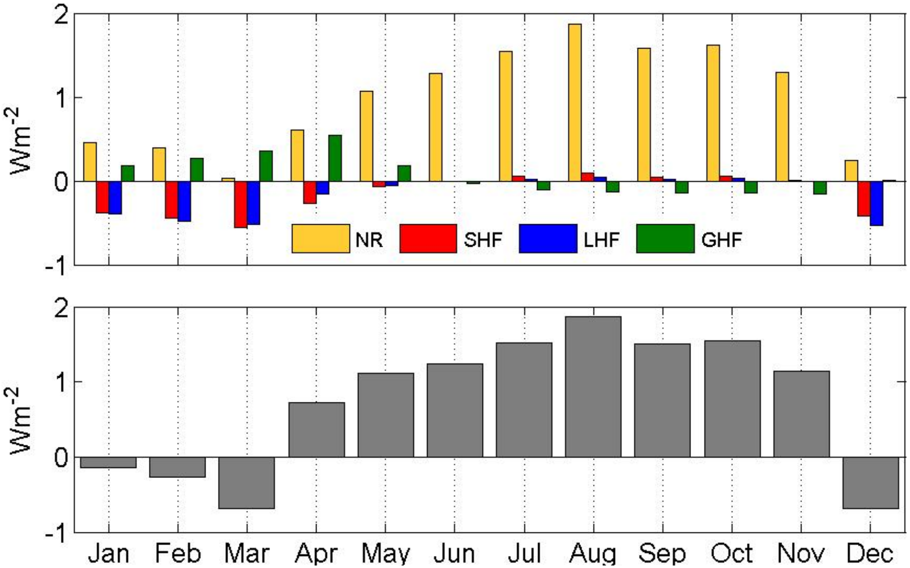

Fig. 7. Mean monthly energy balance components (upper panel) and total energy balance (lower panel). NR denotes net radiation, SHF sensible heat flux, LHF latent heat flux and GHF is ground heat flux. Positive sign indicates a gain of energy at the surface.

TCD

4, 1741–1779, 2010

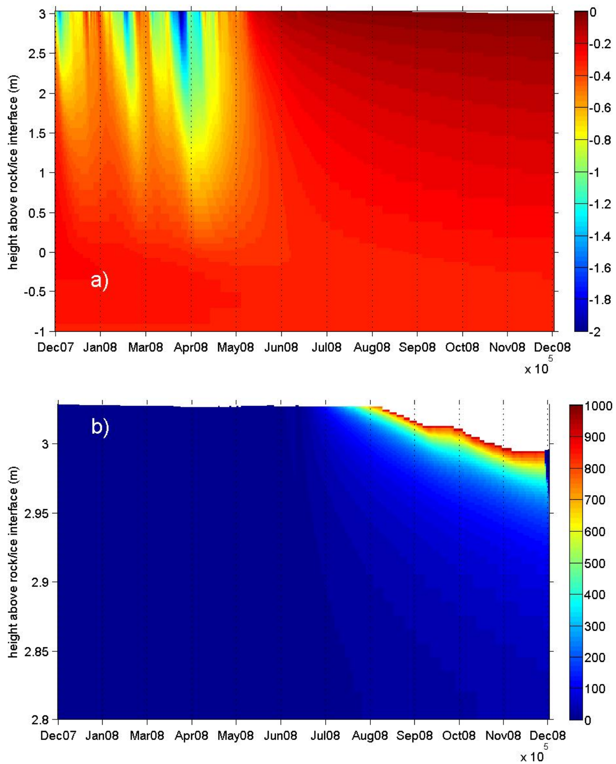

Fig. 8. Time-depth development of ice and rock temperatures within the model domain (upper panel) and liquid water content (kg m^{-3}) in the top 20 cm (lower panel).

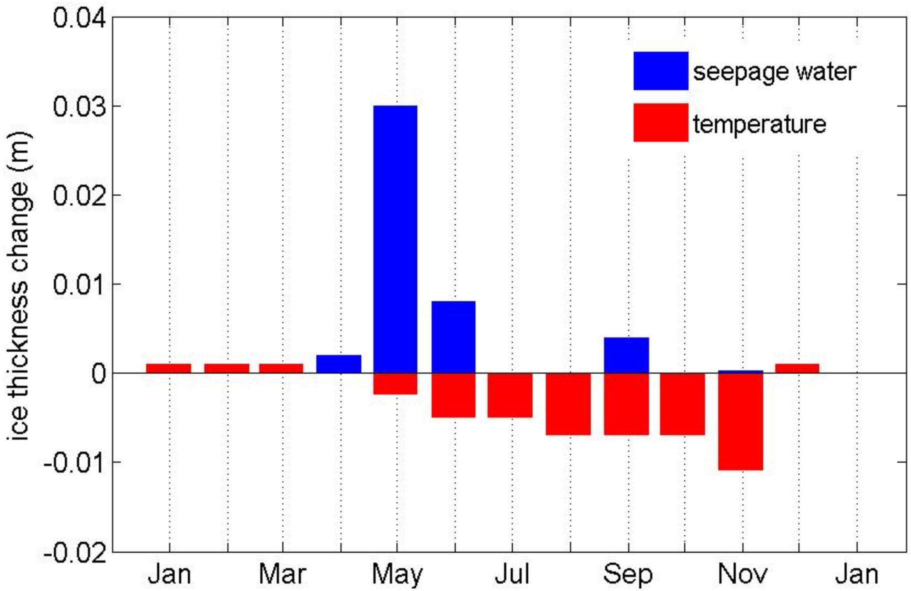

Fig. 9. Mean monthly sensitivity characteristics referring to increased temperature (+1 °C) and input of seepage water (0.05 mm h^{-1}) in respective months. The effect on the mass balance is measured in terms of annual changes in ice thickness compared to the reference run.

TCD
4, 1741–1779, 2010

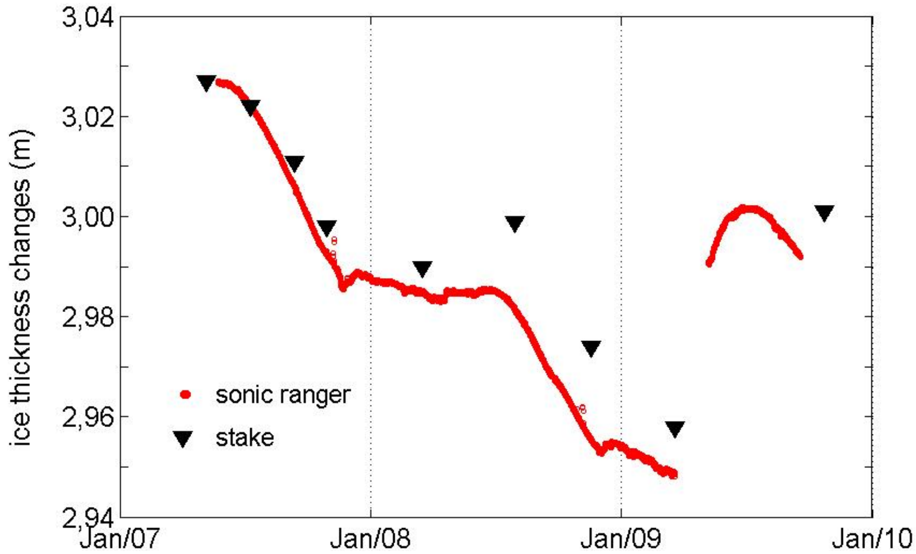

Fig. 10. Measured changes in ice thickness during two successive years indicating a strong influence of seepage water in spring 2009. Dashed lines mark the period of the reference run.

TCD
4, 1741–1779, 2010

Mass and energy balance of ice

F. Obleitner and Ch. Spötl